Journal of Mammalogy, xx(x):1–14, 2017
DOI:10.1093/jmammal/gyx008

Rapid increase in genetic diversity in an endemic Patagonian tuco-tuco following a recent volcanic eruption

Jeremy L. Hsu,* Sharon Kam, Mauro N. Tammone, Eileen A. Lacey, and Elizabeth A. Hadly

Department of Biology, Stanford University, Stanford, CA 94305, USA (JLH, SK, EAH)
Unidad de Investigación Diversidad, Sistemática y Evolución, Centro Nacional Patagónico (CENPAT-CONICET), 9120 Puerto Madryn, Chubut, Argentina (MNT)
Programa de Estudios Aplicados a la Conservación (CENAC-PNNH, CONICET), 8400 Bariloche, Río Negro, Argentina (MNT)
Museum of Vertebrate Zoology and Department of Integrative Biology, University of California, Berkeley, CA 94720, USA (EAL)
Woods Institute for the Environment, Stanford University, Stanford, CA 94305, USA (EAH)
Center for Innovation in Global Health, Stanford University, Stanford, CA 94305, USA (EAH)
Present address of JLH: Chapman University, 1 University Drive, Orange, CA 92866, USA

* *Correspondent: hsu@chapman.edu*

Catastrophic natural events can have profound impacts on patterns of genetic diversity. Due to the typically unpredictable nature of such phenomena, however, few studies have been able to directly compare patterns of diversity before and after natural catastrophic events. Here, we examine the impacts of a recent volcanic eruption in southern Chile on genetic variation in the colonial tuco-tuco (*Ctenomys sociabilis*), a subterranean species of rodent endemic to the area most affected by the June 2011 eruption of the Puyehue-Cordón Caulle volcanic complex. To provide a comparative context for interpreting changes in genetic variation in this species, we also analyze the effects of this eruption on genetic variation in the geographically proximate but more widely distributed Patagonian tuco-tuco (*C. haigi*). Our analyses indicate that while both *C. sociabilis* and *C. haigi* displayed significant post-eruption decreases in population density, the apparent impacts of the eruption on genetic diversity differed between species. In particular, genetic diversity at multiple microsatellite loci increased in *C. sociabilis* after the eruption while no comparable post-eruption increase in *C. haigi* was observed at these loci. No changes in post-eruption diversity at the mitochondrial cytochrome *b* locus were detected for either species. To place these findings in a larger spatiotemporal context, we compared our results for *C. sociabilis* to genetic data from additional modern and ancient populations of this species. These comparisons, combined with Bayesian serial coalescent modeling, suggest that post-eruption gene flow from nearby populations represents the most probable explanation for the apparent increase in post-eruption microsatellite diversity in *C. sociabilis*. Thus, detailed comparisons of pre- and post-eruption populations provide important insights into not only the genetic consequences of a natural catastrophic event, but also the demographic processes by which these changes in genetic diversity likely occurred.

Los eventos naturales catastróficos pueden generar impactos notables en los patrones de diversidad genética. Debido a que estos fenómenos son típicamente impredecibles, muy pocos estudios han podido dedicarse a comparar patrones de diversidad genética antes y después de un evento natural catastrófico. En este trabajo se examina el impacto de la erupción volcánica en junio de 2011 del complejo volcánico Puyehue-Cordón Caulle sobre la diversidad genética del tuco-tuco colonial (*Ctenomys sociabilis*), un roedor subterráneo endémico del área más afectada por la erupción volcánica. A su vez, se examinan los efectos de dicha erupción sobre la diversidad genética del parapátrico tuco-tuco patagónico (*C. haigi*), ampliamente distribuido en el noroeste de Patagonia. Estos análisis indican que, aunque ambas especies muestran un decrecimiento significativo en la densidad poblacional, el impacto de la erupción en la diversidad genética fue diferente entre las especies. Particularmente, en *C. sociabilis* se observó un aumento de la diversidad genética de varios loci de microsatélites luego de la erupción volcánica, mientras que en *C. haigi* no se observó tal aumento. Para el locus mitocondrial

citocromo b no se observó ningún cambio de diversidad genética luego de la erupción volcánica en ninguna de las especies. Para ubicar estos descubrimientos en un contexto temporal más amplio, los resultados de *C. sociabilis* se compararon con datos genéticos de otras poblaciones actuales y antiguas de esta especie. Utilizando modelos bayesianos basados en la teoría serial coalescente, esto análisis sugieren que el flujo genético post-erupción representa la explicación más probable al aumento en la diversidad de microsatélites en *C. sociabilis*. De esta manera, las comparaciones entre poblaciones pre- y post-erupción proporcionan información relevante no solo sobre las consecuencias genéticas de eventos naturales catastróficos, sino también sobre los procesos demográficos que probablemente generaron tales cambios en la diversidad genética.

Key words: *Ctenomys*, genetic diversity, subterranean rodents, volcanic eruption

Catastrophic natural events (e.g., hurricanes, floods, earthquakes) can severely impact genetic diversity in natural populations, with such changes typically occurring within a short period of time relative to the life span of the affected organisms (Pujolar et al. 2011). Such catastrophic events often result in demographic bottlenecks that reduce genetic diversity and alter the selective pressures acting on populations (Akey et al. 2004). However, determining the precise demographic and genetic impacts of catastrophic events is challenging, in part because the generally unpredictable nature of such events often precludes the collection of pre- and post-catastrophic data, thereby necessitating inferences based solely on post-event sampling of populations. Because few studies have directly compared pre- and post-event data, the specific demographic processes underlying genetic responses to catastrophic change remain poorly understood (Beheregaray et al. 2003; Pujolar et al. 2011; Wilmer et al. 2011).

The June 2011 eruption of the Puyehue-Cordón Caulle volcanic complex (40.5°S, 72.2°W; Fig. 1) in southeastern Chile provides a rare opportunity to explore the demographic and associated genetic consequences of a naturally occurring catastrophic environmental event. The eruption continued for more than 2 weeks (Collini et al. 2012), releasing more than 950 million tons of tephra (ash and other organic matter) across northern Patagonia, from the Andean crest eastward to the Atlantic Ocean (Gaitán et al. 2011). The impacts on livestock in the region were substantial, with an estimated 60% decrease in populations of sheep and goats (Wilson et al. 2012). The eruption also impacted nonagricultural taxa; among exotic species, the eruption caused fluoride intoxication and reduced longevity in European red deer (*Cervus elaphus*—Flueck and Smith-Flueck 2013; Flueck et al. 2014) as well as significant reductions in the population sizes of introduced vespid wasps (Masciocchi et al. 2012). Native species were also affected, as evidenced by reported reproductive abnormalities in liolaemid lizards (Boretto et al. 2014) and disruptions of both plant–pollinator relationships (Morales et al. 2014) and aquatic invertebrate communities (Lallement et al. 2014). In sum, ash fall from the Puyehue-Cordón Caulle eruption had widespread, diverse, and profound effects on the flora and fauna of northern Patagonia.

Among the native taxa impacted by the ash fall were 2 species of tuco-tucos (Rodentia: Ctenomyidae). Since 1992, the colonial tuco-tuco (*Ctenomys sociabilis*) and the Patagonian tuco-tuco (*C. haigi*) have been the subjects of intensive field research aimed at characterizing the behavior, ecology, and demography

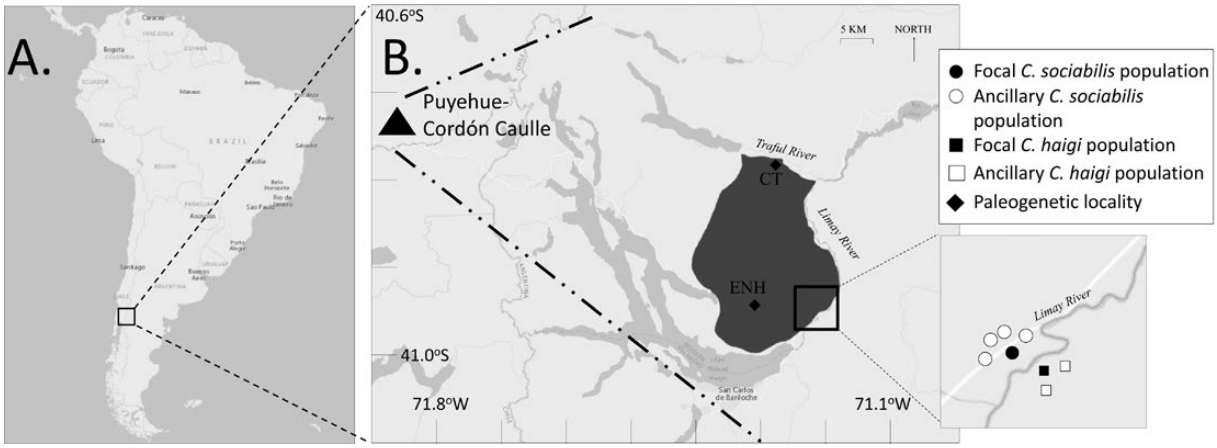

Fig. 1.—A) Map of South America showing inset of field sites. B) Inset depicts the close proximity of the range of *Ctenomys sociabilis* range (shaded) to the Puyehue-Cordón Caulle volcanic complex. The range of the parapatric congener *C. haigi* is located across the Limay River. The dashed-dotted line shows approximate cone of tephra from the 2011 eruption. Focal and ancillary populations of *C. sociabilis* (circles) and *C. haigi* (squares) are also indicated. Closed shapes indicate focal populations of *C. sociabilis* (closed circle, at Estancia Rincon Grande) and *C. haigi* (closed square, at Estancia San Ramon). Non-focal populations surround the focal populations and are represented by open circles (*C. sociabilis*) and open squares (*C. haigi*). The localities of paleogenetic samples at Cueva Traful (CT) and Estancia Nahuel Huapi (ENH) are indicated with diamonds.

of each species (Lacey et al. 1997, 1998, 1999; Hadly et al. 2003; Chan et al. 2005; Lacey and Ebensperger 2007; Chan and Hadly 2011). As a result, data from these herbivorous, burrow-dwelling taxa provide a rare opportunity to directly assess the demographic and genetic consequences of the Puyehue-Cordón Caulle eruption. Both species breed once per annum and have a generation time of 1 year (Chan et al. 2006). The colonial tuco-tuco, listed as critically endangered by the IUCN, is endemic to a less than 1,500-km^2 area in southern Neuquen Province, Argentina, that includes the western side of the Limay River Valley and adjacent hills (Fig. 1). In contrast, the parapatric *C. haigi* is widely distributed in the eastern Limay Valley and adjacent portions of Río Negro Province, where it occurs in habitats similar to those occupied by *C. sociabilis* (Lacey and Wieczorek 2004). Despite their close geographic proximity and use of similar habitats, the 2 species differ markedly in their behavior: *C. haigi* is solitary, with each adult occupying its own burrow system, while *C. sociabilis* is the only ctenomyid species that has been demonstrated to live in groups (Lacey et al. 1997, 1998). The long-term focal study populations for these species are located in the Limay Valley (Fig. 1), approximately 100 km east of the Puyehue-Cordón Caulle volcanic complex. As a result, both study sites experienced substantial (3–5 cm) ash fall following the 2011 eruption (Masciocchi et al. 2012; Wilson et al. 2013) and both study populations experienced a significant post-eruption decrease in population density (E. A. Lacey, pers. obs.).

Here, we examine the impacts of the 2011 eruption on the genetic variation in the populations of *C. sociabilis* that have been the focus of long-term demographic research. Specifically, we compare levels of microsatellite and cytochrome *b* genetic variation in pre- and post-eruption samples from these populations to assess the genetic consequences of this event. To provide a comparative context for theses analyses, we also analyze pre- and post-eruption variation in the focal study population of *C. haigi*. To place our findings in a larger spatiotemporal framework, we also consider pre-eruption data on genetic variation from several additional populations of each species as well as available mitochondrial paleogenetic data from these taxa, allowing us to contrast short-term changes in genetic diversity with more extended responses to environmental change. Finally, we use Bayesian serial coalescent modeling informed by demographic and genetic data from our study to identify population processes that may have contributed to post-eruption changes in genetic diversity. Collectively, these analyses offer important insights into the demographic processes underlying the immediate genetic consequences of a natural catastrophic event.

Materials and Methods

Sample collection and demographic analysis.—Non-destructive tissue samples from *C. sociabilis* and *C. haigi* were collected during the austral summers (November–January) of 1993–1998 and 2011–2013 (designated as pre- and post-eruption, respectively), following the trapping and sampling procedures described in Lacey (2001). We analyzed samples from 85 individuals (54 pre-eruption, 31 post-eruption) from the focal population of *C. sociabilis* at Estancia Rincon Grande and 62 individuals (45 pre-eruption, 17 post-eruption) from the focal population of *C. haigi* at Estancia San Ramon (Table 1; Fig. 1). These localities have been the focus of an intensive annual mark–recapture program since 1992 and thus genetic analyses of samples from these populations could be linked to pre- and post-eruption demographic information from the same animals (E. A. Lacey, pers. obs.). To gain a more comprehensive picture of pre-eruption genetic variation in these focal populations, we also included data from an additional 20 individuals per species from the pre-eruption time period; genotypes for these individuals were generated as part of Lacey (2001). Given that sampling between the pre- and post-eruption periods was

Table 1.—Summary of *Ctenomys sociabilis* and *C. haigi* samples analyzed by time period and population; totals include 20 pre-eruption samples from each focal population previously genotyped by Lacey (2001). A) Number of individuals sampled and used in microsatellite and cytochrome *b* analyses. B) Age distribution of samples included in each population for microsatellite analyses. Samples from ancillary populations were not collected after the eruption due to the difficulty of accessing these sites under post-eruption conditions.

	C. sociabilis populations		*C. haigi* populations	
	Focal	Ancillary	Focal	Ancillary
A) Number of individuals sampled				
Pre-eruption (1993–1998)				
Total samples	74	42	65	25
Samples included for microsat analyses	74	42	60	25
Samples included for cytochrome *b* analyses	14	0	13	0
Post-eruption (2011–2013)				
Total samples	31	0	17	0
Samples included for microsat analyses	31	0	17	0
Samples included for cytochrome *b* analyses	31	0	17	0
B) Age distribution of individuals sampled				
Pre-eruption (1993–1998)				
Adults	57	4	38	23
Juveniles	17	38	22	2
Post-eruption (2011–2013)				
Adults	5	0	10	0
Juveniles	26	0	7	0

separated by over a decade, none of the individuals included in the pre-eruption sampling were present during or after the eruption. To assess the potential impacts of including individuals of different ages in our analyses, we segregated the data set by age (adult versus juvenile), ran separate analyses for each age class, and then compared the results from these partitioned data sets to those from the full data set.

To place our comparisons of genetic variation in a broader spatial context, we included samples from 4 additional populations (hereafter referred to as ancillary populations) of *C. sociabilis* (n = 42 individuals) and 2 additional populations of *C. haigi* (n = 25 individuals) collected between 1993 and 1998, during the pre-eruption time period (Fig. 1; Table 1). We defined a population as a contiguous set of burrows that was spatially distinct from other collections of burrows. These populations were clearly defined ecologically, given the distance (~1 km) between clusters. The ancillary populations were not sampled after the eruption due to difficulties accessing these sites under post-eruption conditions. Thus, direct comparisons of pre- and post-eruption genetic variation were not possible for these localities. We have included data from these ancillary localities, however, because they provide a broader spatial perspective on pre-eruption genetic variation. The specific subsets of samples used in each analysis are indicated in Table 1. Similarly, to provide a broader temporal context for our data, we included previously published data on mitochondrial cytochrome *b* variation among 34 *C. sociabilis* and 31 *C. haigi* (Chan et al. 2006) samples dating back to 12,000 years before present.

This study was carried out in compliance with all local, national, international, and institutional regulations. Permits for fieldwork were granted by the Delegación Tecnica Regional Patagonia de Parques Nacionales Argentinas and Provincia Rio Negro. All activities involving live animals were approved by the Animal Care and Use Committee at the University of California, Berkeley, and were consistent with the guidelines of the American Society of Mammalogists for the use of wild mammals in research (Sikes et al. 2016).

DNA extraction and microsatellite amplification.—DNA was extracted from tissue samples using a DNeasy Blood and Tissue extraction kit (Qiagen, Valencia, California). The success of extractions was assessed via polymerase chain reaction (PCR), with negative controls included to test for contamination. Following extraction, we amplified 5 *C. sociabilis*-specific microsatellite loci using published primers from Lacey et al. (1999) and Lacey (2001). These loci were chosen because 1) they represent the only species-specific loci known to be variable in *C. sociabilis* (Lacey 2001), and 2) they were successfully genotyped in greater than 80% of our samples, thus minimizing the potential for biases in the resulting data on genetic variation. Although other loci have been genotyped for members of both species, previous analyses indicate that *C. sociabilis* is monomorphic at these loci (Lacey et al. 1999; Lacey 2001), and thus analyses of these markers were not expected to be informative regarding the effects of the 2011 eruption. The general reaction protocol for PCR amplification and locus-specific annealing temperatures used were the same as those specified in Lacey et al. (1999), Lacey (2001), and Chan et al. (2005).

Microsatellite genotyping and scoring.—Following PCR amplification of microsatellite loci, all samples were sent to Molecular Cloning Laboratories (ABI 3730XL; South San Francisco, California) or the Stanford Protein and Nucleic Acid facility (ABI 3130XL; Stanford, California) for genotyping. The resulting fragment lengths were analyzed and individual genotypes were assigned using Geneious Pro (Biomatters Limited, Auckland, New Zealand). All genotypes were determined independently by at least 3 different individuals; any discrepancies in allele assignments were resolved by re-genotyping the locus for the sample in question. To further ensure accurate scoring of genotypes, approximately 20% of DNA extracts from our post-eruption samples from *C. sociabilis* were re-amplified or re-genotyped. In addition, multiple PCR products were sequenced by ElimBio Pharmaceuticals (Hayward, California) to confirm the presence of a microsatellite repeat; comparing these data against reference sequences in GenBank confirmed that flanking sequences matched those from *C. sociabilis* and *C. haigi*. Finally, all samples were independently amplified, genotyped, and scored by the Stanford Protein and Nucleic Acid facility to provide additional verification; as a result, all samples in our data set were genotyped and scored in duplicate. The resulting data were examined for evidence of null alleles and allelic dropout using MicroChecker v2.2.3 (van Oosterhout et al. 2004). Based on these analyses (van Oosterhout et al. 2004), all loci were retained for further analyses. We then pooled our data with genotypes for 20 pre-eruption samples from each focal population obtained from Lacey (2001) to generate a more robust data set for analyses of genetic variation. To ensure consistency across studies, a randomly chosen subset of these samples analyzed by Lacey (2001; n = 6) was re-genotyped to confirm allelic assignments.

Power analyses of microsatellite data.—Given the relatively limited number of microsatellite loci genotyped, we used POWSIM (Ryman and Palm 2006) to infer the statistical power of our analyses. POWSIM employs a series of empirical parameters (number of loci, number of alleles per locus, allele frequencies, and sample size), a specified number of populations, and a predetermined level of genetic diversity to estimate the power of a data set to detect genetic differentiation. POWSIM analyses were run using a range of predefined F_{ST} values (0.01, 0.025, and 0.05) to determine the power of our microsatellite data to detect potential differences in pre- and post-eruption variation in each focal population as well as to detect differences between the focal and ancillary populations of each study species.

In addition, to ensure that differences in sample sizes did not bias our comparisons of pre- and post-eruption data, we conducted a bootstrapping analysis of microsatellite genotypes using a custom R script (available upon request). For the focal population of each study species, the number of pre-eruption samples analyzed (*C. sociabilis*, n = 74; *C. haigi*, n = 65) was greater than the number of post-eruption samples (*C. sociabilis*, n = 31; *C. haigi*, n = 17). Accordingly, we randomly subsampled

31 and 17 pre-eruption samples for *C. sociabilis* and *C. haigi*, respectively. This subsampling was repeated 1,000 times, after which bootstrapped values were compared to the observed values calculated for the entire data set to determine if estimates of microsatellite variation were impacted by sample size.

Analyses of microsatellite variation.—To characterize microsatellite variation in the study species, we tested for departures from Hardy–Weinberg equilibrium and calculated values for standard population genetic parameters (observed and expected heterozygosity, F_{IS}, F_{ST}, allelic richness and variance, genotypic differentiation, gene diversity) using GenePop (Raymond and Rousset 1995), FSTAT (Goudet 1995), and Arlequin (Excoffier and Laval 2005). Allelic richness was calculated per locus and population with a minimum sample size of 16 individuals. All statistically significant outcomes for these and other analyses are explicitly indicated in the text of the results or associated figures.

To evaluate spatial structuring of pre-eruption genetic diversity, we examined all microsatellite data (pre- and post-eruption) from each focal population as well as data from the associated ancillary populations for each species. Samples from focal and ancillary populations had been collected during the same range of pre-eruption years (1993–1998). To explore potential temporal genetic differentiation within the focal populations, we also included data from these populations collected after the eruption (2011–2013). Assessments of potential spatial and temporal genetic differentiation among conspecifics were conducted using the analysis of molecular variance (AMOVA) test, as implemented in Arlequin. To determine if patterns of post-eruption genetic variation in *C. sociabilis* and *C. haigi* revealed evidence of a recent decrease in population size, we examined the microsatellite data for signatures of population bottlenecks following the methods of Cornuet and Luikart (1996) and Garza and Williamson (2001). Specifically, we tested for both heterozygosity excess and changes in the *M*-ratio, which represents the ratio of the number of alleles to the range of allele sizes (Garza and Williamson 2001). Reductions in population size are expected to reduce the number of alleles more rapidly than the range of allele sizes; thus, this ratio can reveal evidence of past bottlenecks (Garza and Williamson 2001; Peery et al. 2012).

The use of 2 analytical methods that rely on different signals of change in a putatively bottlenecked population provides additional power for detecting the effects of such historical events. We used BOTTLENECK v1.2.02 (Piry 1999) to test for heterozygosity excess in each post-eruption focal study population. We employed both a stepwise mutation model (SMM) and a 2-phase mutation model (TPM) with the proportion of single mutations set at multiple values (80%, 85%, 90%, 95%) considered appropriate for microsatellite loci (Funk et al. 2010). We set the variance in mutation lengths at 0.36 and ran each test for 1,000 iterations. The significance of any apparent excess in heterozygosity was assessed using a Wilcoxon signed-rank test. *M*-ratios were calculated with Arlequin, with critical values for this parameter determined using *M*-crit (Garza and Williamson 2001). We set the average size of multistep mutations to be 3.5 with 10% multistep mutations in the model. Based on estimates provided by Chan et al. (2006), we estimated the effective size for each focal population to be 300 individuals. We varied the mutation rate from 10^{-3} to 10^{-4}, which corresponds to the range of mutation rates typically found at microsatellite loci (Mapelli et al. 2012). Based on the equation $\theta = 4N_eM$, this thus produced values of θ ranging from 1.2 to 12. Critical *M*-ratio values based on these values of theta were then compared to the observed *M*-ratio values to determine the significance of apparent signatures of bottlenecks.

Mitochondrial DNA sequencing and analyses.—To provide a potentially different perspective on post-eruption changes in genetic variation and to enable comparisons of our pre- and post-eruption samples with paleogenetic information from the same locus in the study species (Hadly et al. 2003; Chan et al. 2005), we amplified portions of the mitochondrial cytochrome *b* locus (*C. sociabilis*, $n = 900$ base pairs [bp]; *C. haigi*, $n = 600$ bp) across a subset of samples from both species (*C. sociabilis*, $n = 45$; *C. haigi*, $n = 30$; Table 1). Amplification was performed using primers MVZ05 (Smith 1998) and MVZ108 (Chan et al. 2005), which were designed to encompass the regions of this locus that had been sequenced previously from paleogenetic samples (Chan et al. 2006). PCR conditions followed those of Chan et al. (2005). Sequencing of these products was completed by ElimBio Pharmaceuticals, after which the resulting sequences were cleaned, assembled, and aligned using SeqMan (Lasergene Suite from DNAStar, Madison, Wisconsin). Putative haplotypic variants were verified via visual inspection of the associated electropherograms. All haplotypes generated were compared to cytochrome *b* sequences for *C. sociabilis* and *C. haigi* available in GenBank. All novel sequences generated were accessioned to GenBank (accession IDs KY013598–KY013609).

To characterize mitochondrial sequence diversity and examine potential signals of demographic change in each species, we used Arlequin to calculate Tajima's *D*, Fu's *F*, F_{ST} and F_{IS} values, θ_S (as defined by Watterson 1975), and θ_π (as defined by Tajima 1983) from our cytochrome *b* sequences. Arlequin was also used to conduct an AMOVA for each species to assess relative variation within versus among populations. To examine potential differences in haplotype distributions over time, we generated haplotype network maps using TempNet (Prost and Anderson 2011), which allows the temporal partitioning of heterochronous sequence data. We generated a temporal haplotype network with the pre- and post-eruption samples from the focal populations as distinct temporal layers. To provide a deeper temporal perspective on haplotypic variation, we pooled cytochrome *b* sequence data generated by this study with paleogenetic data from Hadly et al. (2003) and Chan et al. (2006) to examine potential changes in haplotypic variation over the last 12,000 years. These analyses were completed using only those portions of the modern cytochrome *b* sequence data (*C. sociabilis*, 398 bp; *C. haigi*, 288 bp) that corresponded to the paleogenetic sequences for each study species. Comparisons of modern and paleogenetic data were conducted using TempNet.

Bayesian serial coalescent modeling.—To explore how potential demographic processes such as changes in population size, mutation rate, and migration may have contributed to changes in genetic diversity over time, we used BayeSSC (Anderson et al. 2005) with an approximate Bayesian computation (ABC) framework to simulate the impacts of a bottleneck on the focal study population of *C. sociabilis*. We used demographic estimates from trapping records (E. A. Lacey, pers. obs.) and from Chan et al. (2006) to simulate a 52.9% decrease in population size 2 generations prior to the collection of our data set; this timeline was chosen to encompass all possible generations present at the time of our post-eruption sample. N_e prior to the bottleneck was set at 50 individuals, a conservative estimate based on our demographic data. We simulated the effects of the eruption for the microsatellite data, using a mutation rate of 0.001 mutations/generation. This figure represents the upper end of the range of mutation rates considered biologically feasible for microsatellites (Mapelli et al. 2012). We ran simulations for 1,000,000 samples and calculated the percentage of runs that displayed a change in heterozygosity matching the change observed post-eruption in our empirical data set.

We then explored the effects of changes in population size, mutation rate, and migration rate on post-eruption genetic diversity. For the microsatellite data set, we varied the prior distributions for these parameters in our simulations, which were again run for 1,000,000 samples. We applied an ABC framework with a 5% rejection threshold for the posterior distributions to determine the most likely estimates (MLEs) for the priors. Specifically, we compared 4 summary statistics (pre- and post-eruption observed heterozygosities and allelic variances) from the empirical data set to our posterior distributions to determine the MLE for each prior. We ran analyses using the average observed heterozygosity and allelic variance calculated across all microsatellite loci as well as the observed heterozygosity and allelic variance from the 2 loci (Sociabilis 4 and Sociabilis 7) that had the largest and smallest post-eruption changes in heterozygosity, respectively (see "Results"). Use of these extremes provided an upper and lower bound for our MLEs of priors. We varied the uniform distributions used for priors to assess the consistency of the resulting posterior distributions and MLE values. In the event of large variations in MLE values, we assessed the fit of standard statistical distributions (uniform, exponential, normal, and gamma distributions) to the posterior using negative log likelihood and Akaike Information Criteria (AIC) values and, if necessary, modified the associated prior.

The 1st parameter examined was population size, which was set as a uniform prior ranging from 0 to 5,000 individuals, a conservative range chosen to encompass any biologically feasible population size for this species. Next, to explore the impact of mutation rate, we ran simulations with the mutation rate set as a prior and with a constant population size (pre-eruption estimate of 50 individuals); for these runs, we used a uniform distribution of mutation rates ranging from 0 to 0.3, which encompasses the range of substitution rates reported for mammalian microsatellites (Yue et al. 2002; Mapelli et al. 2012). Finally, to examine the impacts of migration, we repeated these simulations but allowed for the presence of a second population, representing the pooled ancillary populations for the species. For these analyses, we set the forward-in-time migration rate from the neighboring localities into the focal population of *C. sociabilis* as a prior with a uniform distribution. We varied 1) N_e for the neighboring localities (range = 50 to 10,000 individuals), and 2) forward-in-time migration rate from the focal population to neighboring localities (migration rate ranged from 0 to 0.1). All simulations were run for 100,000 samples. While simulations were run backward in time, all migration rates here are presented as forward in time for clarity.

Results

Microsatellite genotypes were largely consistent across multiple independent rounds of amplification, genotyping, and scoring, providing verification of our results (individual microsatellite genotypes are available by request). Within species, we found no differences in microsatellite variation between data sets containing adults only, juveniles only, or adults and juveniles together and thus all subsequent analyses were conducted using all samples for each species. Our bootstrapping analyses provided evidence that sample size did not affect estimates of variation: with the exception of 1 locus in *C. haigi* (Sociabilis 1), all measures of heterozygosity in our pre-eruption samples fell within 95% confidence intervals for estimates of heterozygosity obtained via bootstrapping, suggesting that differences in sample sizes for pre- and post-eruption data sets did not impact estimates of genetic diversity. The 1 locus that differed in *C. haigi* (Sociabilis 1) had a mean bootstrapped heterozygosity value that was less than 0.01 different from the empirical value of heterozygosity across all samples, and thus was still included in analyses to obtain more robust results. Accordingly, we included all available pre- and post-eruption genotypes in our analyses of microsatellite variation.

Our POWSIM results indicated that our microsatellite data set had sufficient power to detect genetic differentiation. A power of 0.80 or greater has been suggested as the threshold for providing adequate statistical power (Cohen 1988); we found that the power of our comparisons between pre- and post-eruption variation in our focal populations as well as between the focal and ancillary populations in each species were largely greater than this threshold. Specifically, given a predefined F_{ST} value of 0.025 or greater, the POWSIM analyses indicated that the data set for *C. sociabilis* had a power of 0.75 to detect genetic differentiation (all values provided from chi-squared test). Statistical power rose to 0.91 if these analyses were run with $F_{ST} > 0.05$. Estimated power of the data set from the focal population of *C. haigi* was greater, with a power of 0.99 for $F_{ST} > 0.025$ and a power of 1.00 for F_{ST} value > 0.05. When the ancillary populations for each species were included, power was 0.93 and 1.00 for *C. sociabilis* and *C. haigi*, respectively, for $F_{ST} > 0.025$. Power rose to 0.99 and remained at 1.00 for *C. sociabilis* and *C. haigi*, respectively, for $F_{ST} > 0.05$. Given that observed values of F_{ST} (see results section below) for both

study species were greater than those used in the POWSIM analyses, and given that the resulting estimates of power were generally greater than the 0.80 threshold, our data set appeared to be sufficient to detect genetic differentiation in both study species. Thus, we retained all microsatellite loci in our analyses and used these loci to compare temporal and genetic divergence among populations.

Temporal changes in cytochrome b diversity.—We analyzed cytochrome *b* sequences for 45 individuals from the focal population of *C. sociabilis* and 30 individuals from the focal population of *C. haigi* (Table 1); this sample included data from 14 *C. sociabilis* and 13 *C. haigi* sampled during the pre-eruption time period (1993–1998) that had been sequenced previously by Lacey (2001) and Hadly et al. (2003). Only a single cytochrome *b* haplotype was detected in the focal population of *C. sociabilis* both before (1993–1998, $n = 17$) and after (2011–2013, $n = 26$) the 2011 eruption. In contrast, the focal population of *C. haigi* was characterized by multiple haplotypes in both time periods (5 haplotypes pre-eruption; 10 haplotypes post-eruption; Fig. 2). Expansion of our analyses to include cytochrome *b* genotypes from paleogenetic samples from each species (Chan and Hadly 2011) revealed a general pattern of declining haplotype diversity in *C. sociabilis* over the past 10,000 years (Supplementary Data SD1A); in comparison, *C. haigi* has maintained relatively consistent levels of haplotype diversity over this same time period (Supplementary Data SD1B).

Patterns of nucleotide diversity at the cytochrome *b* locus paralleled interspecific differences in haplotypic diversity. With only 1 haplotype detected in both pre- and post-eruption samples, there was no change in diversity in *C. sociabilis*. In contrast, analyses of haplotypes from the focal population of *C. haigi* revealed considerably greater levels of nucleotide diversity for all measures considered. Prior to the eruption, θ_S was 1.66 and θ_π was 1.24; post-eruption, these values were 3.01 and 2.88, respectively. Values for Tajima's *D* (pre-eruption = −0.92, $P = 0.22$; post-eruption = −0.17, $P = 0.47$) were negative, as were values for Fu's F_s (pre-eruption = −18.1; post-eruption = −18.55; P for both < 0.005). AMOVA analyses revealed that 97.8% of the variation detected occurred within the study population, with the remainder occurring between the pre- and post-eruption subsets of this population. The F_{ST} between pre- and post-eruption samples was 0.0218 ($P = 0.25$). In sum, these analyses indicate that cytochrome *b* haplotypes were characterized by considerably more nucleotide diversity in *C. haigi* than in *C. sociabilis*.

Temporal changes in microsatellite diversity.—In *C. sociabilis*, only 1 microsatellite locus (Sociabilis 4) deviated significantly from Hardy–Weinberg expectations (Hardy–Weinberg probability tests, 1000 iterations; $P < 0.005$; Table 2A) in the pre-eruption focal population, although there was evidence of a significant departure from neutral expectations when data from all loci were considered together (Fisher's exact test, $P < 0.05$). After the 2011 eruption, no loci deviated from Hardy–Weinberg expectations in this population (Table 2A), and similarly there was no deviation from Hardy–Weinberg expectations when data from all loci were considered together (Fisher's exact test, $P = 0.18$). Prior to the eruption, 4 of 5 microsatellite loci displayed positive values of F_{IS}; in contrast, all post-eruption values of F_{IS} were negative (Table 2A; all $P > 0.05$).

The number of alleles detected in the focal population of *C. sociabilis* did not change before versus after the eruption for 2 of 5 loci (Sociabilis 1 and 5) and decreased by only a single allele after the eruption at each of the remaining loci

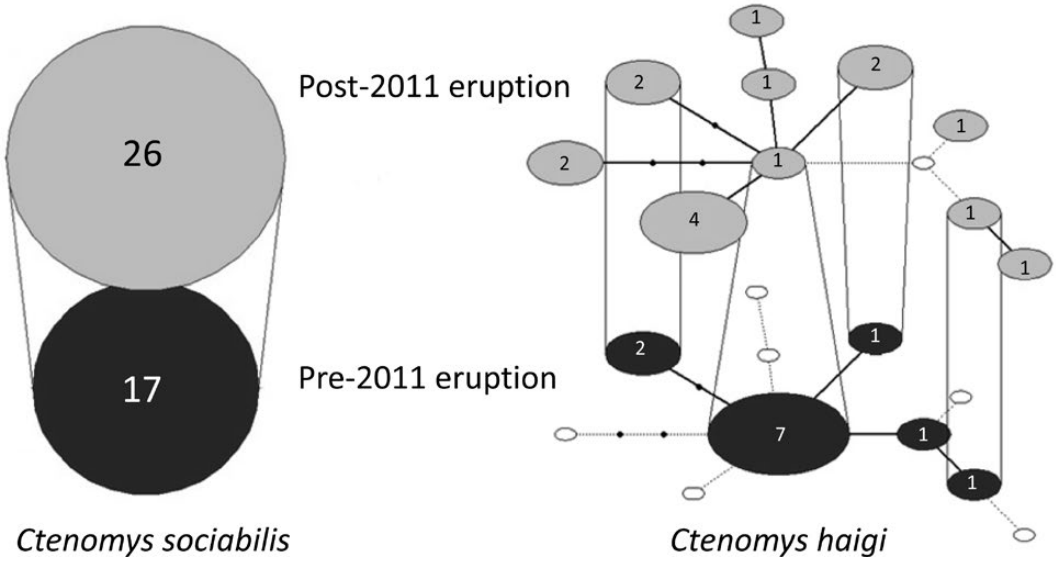

Fig. 2.—Haplotype networks for cytochrome *b* in the focal populations of *Ctenomys sociabilis* (left; 900 bp) and *C. haigi* (right; 600 bp). Each circle represents a unique haplotype, with the size of the circle indicating the relative frequency of that haplotype (number of individuals provided in the center of each circle). Nodes represent the number of base pair differences between haplotypes. The bottom layers (dark gray) for both species depict the haplotype network prior to the 2011 eruption (1993–1998), while the top layers (light gray) depict the network following the 2011 eruption (2012–2013). Solid lines spanning the 2 layers connect any haplotypes that are found in both time periods. Open circles show "missing" haplotypes; these are haplotypes found at other times but not present in the designated time period.

Table 2.—Summary of microsatellite variation in the focal population of each study species. Results are shown for Hardy–Weinberg probability tests, F_{IS} values (Weir and Cockerham estimate), gene diversity, and expected heterozygosity across the 5 microsatellites for A) the pre- and post-eruption focal population of *Ctenomys sociabilis* and B) the pre- and post-eruption focal population of *C. haigi*. HWE = Hardy–Weinberg equilibrium.

Locus	HWE *P*-value		F_{IS} estimates		Gene diversity		Heterozygosity (H_E)		Allelic richness (# alleles)	
	Pre	Post	Pre	Post	Pre	Post	Pre	Post	Pre	Post
A) Microsatellite variation in *C. sociabilis*										
Sociabilis 1	0.384	0.291	0.100	–0.261	0.150	0.344	0.150	0.345	1.953 (2)	2.000 (2)
Sociabilis 4	0.000	0.234	0.547	–0.429	0.245	0.438	0.244	0.444	2.389 (3)	2.000 (2)
Sociabilis 5	0.660	0.636	0.041	–0.152	0.261	0.389	0.261	0.390	1.998 (2)	2.000 (2)
Sociabilis 6	1.000	0.359	–0.007	–0.246	0.298	0.432	0.298	0.434	2.228 (3)	2.000 (2)
Sociabilis 7	1.000	0.060	0.028	–0.410	0.319	0.422	0.319	0.425	2.000 (3)	2.000 (2)
B) Microsatellite variation in *C. haigi*										
Sociabilis 1	0.337	0.436	0.017	0.020	0.821	0.829	0.821	0.829	7.213 (9)	7.000 (7)
Sociabilis 4	0.495	0.820	–0.016	0.033	0.627	0.608	0.627	0.608	4.492 (5)	4.882 (5)
Sociabilis 5	0.402	0.805	0.070	–0.044	0.723	0.846	0.722	0.847	6.792 (10)	6.941 (7)
Sociabilis 6	0.476	0.013	–0.015	0.078	0.752	0.827	0.752	0.825	8.561 (13)	7.879 (9)
Sociabilis 7	0.581	0.779	0.068	–0.062	0.855	0.831	0.854	0.832	9.240 (12)	8.763 (9)

(Sociabilis 4, 6, and 7). Similarly, pre- and post-eruption allelic richness did not change appreciably for Sociabilis 1, 5, and 7 and decreased only modestly for Sociabilis 4 and 6 (Table 2A). Comparisons of pre- and post-eruption genotypes revealed significant temporal differentiation at only 1 locus (Sociabilis 1, Fisher's exact *G*-test, $P < 0.05$). In contrast, observed heterozygosity increased significantly after the eruption (Fisher's combined probability test, $P < 0.05$); this pattern was evident for all loci genotyped and significant for 2 loci (Fig. 3A). Values of gene diversity for all loci were greater after the eruption, with mean diversity across all loci increasing from 0.23 to 0.32 (Table 2A). Similarly, estimates of θ_H increased after the eruption for all loci. Although AMOVA analyses revealed that only 4.53% of microsatellite variation was due to temporal differences among samples, comparisons of pre- and post-eruption data sets indicated small but statistically significant temporal population subdivision ($F_{ST} = 0.055$, $P < 0.05$). Thus, these analyses indicate that microsatellite heterozygosity and most associated measures of genetic diversity in the focal population of *C. sociabilis* were greater after the eruption.

Applications of the same analyses to microsatellite data from the focal population of *C. haigi* revealed a substantially different pattern of pre- versus post-eruption genetic diversity. Prior to the eruption, none of the 5 loci examined revealed significant departures from Hardy–Weinberg expectations; post-eruption, only 1 locus (Sociabilis 6) deviated from Hardy–Weinberg expectations (Table 2B). Across all loci, no evidence of significant departure from Hardy–Weinberg expectations was found for either pre- or post-eruption data sets (Fisher's exact test, pre-eruption $P = 0.63$; post-eruption $P = 0.48$). During both time periods, 2 of 5 loci were characterized by negative F_{IS} values, although the identities of these loci differed for pre- versus post-eruption data sets (Table 2B).

The number of alleles detected in the focal population of *C. haigi* decreased after the eruption for 4 of the 5 loci examined; differences in allelic richness were generally small pre- versus

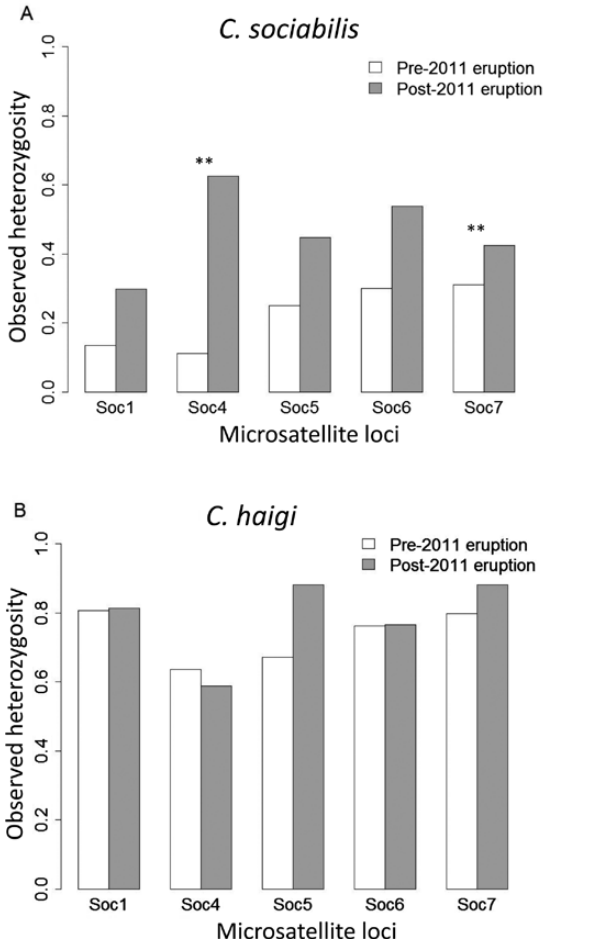

Fig. 3.—Microsatellite variation in A) *Ctenomys sociabilis* and B) *C. haigi*. Graphs depict observed heterozygosity at 5 identified microsatellite loci before (pre-eruption population: 1993–1998) and after (post-eruption population: 2011–2013) the June 2011 volcanic eruption; locus names are abbreviated using Soc followed by the locus number. ** indicates significance at $P < 0.01$ level, Fisher's exact test.

post-eruption, with the exceptions of loci Sociabilis 6 and 7 (Table 2B). There was no consistent pattern of change in gene diversity across time periods, with the largest changes occurring at 3 loci (Sociabilis 5, 6, and 7; Table 2B). Although observed heterozygosity did not differ consistently or significantly before versus after the eruption (Fig. 3B), genotypic diversity at each locus was reduced in the post-eruption samples (Fisher's exact *G*-test, all $P < 0.05$). AMOVA analyses indicated that only 2.39% of microsatellite variation was due to temporal differences among samples. Although temporal differences in allelic frequencies estimated by F_{ST} were low, the difference in this statistic was significant ($F_{ST} = 0.024$, $P < 0.05$). Thus, while *C. sociabilis* was characterized by significant temporal partitioning of microsatellite variation and generally greater microsatellite diversity after the eruption, *C. haigi* displayed no evidence of strong temporal partitioning or greater microsatellite diversity after the eruption.

Tests for population bottlenecks.—A significant excess of heterozygosity was detected for the post-eruption samples of *C. sociabilis* (Wilcoxon signed-rank test; 2-phase model with 80% proportion of single mutations; $P < 0.05$). In contrast, no such excess was detected for the post-eruption population of *C. haigi* (Wilcoxon signed-rank test; 2-phase model with 80% proportion of single mutations; $P = 0.41$). These patterns were consistent when we varied the percentage of single mutations allowed as well as when we repeated analyses using a single mutation model (*C. sociabilis*, $P < 0.05$; *C. haigi*, $P = 0.92$). *M*-ratio tests (Cornuet and Luikart 1996) revealed that for *C. sociabilis*, observed *M*-ratios for all loci were below critical *M*-values for all estimates of θ employed (Table 3). In contrast, for *C. haigi*, only 1 locus (Sociabilis 5) was characterized by an *M*-ratio below the associated critical value. Collectively, these analyses indicate that the 2 focal populations exhibited different genetic signals of recent demographic history, with only *C. sociabilis* displaying patterns of microsatellite variation consistent with a recent population bottleneck.

Table 3.—Tests for population bottlenecks in *Ctenomys sociabilis* and *C haigi*. Comparisons of observed *M*-ratios to critical values of *M* for A) the post-2011 eruption focal population of *C. sociabilis*, and B) the post-2011 eruption focal population of *C. haigi*. Critical *M*-values were computed with a range of values of θ ($4N_e\mu$) ranging from 1.2 to 12, which factors in an effective population size of 300 and a range of μ from 10^{-3} to 10^{-4}. An asterisk (*) indicates significance at the $P < 0.05$ level because critical *M*-values represent the point where 95% of *M*-ratios at equilibrium will be above that critical value. A dash (-) represents nonsignificant values. Critical *M*-values are not repeated after the 1st row since they are the same for each locus, given identical number of samples, loci, and parameters in the model.

Locus	*M*-ratio	θ = 1.2	θ = 5	θ = 10	θ = 12
A) Population bottleneck tests for *C. sociabilis*					
Sociabilis 1	0.286	0.717*	0.660*	0.639*	0.637*
Sociabilis 4	0.500	*	*	*	*
Sociabilis 5	0.222	*	*	*	*
Sociabilis 6	0.250	*	*	*	*
Sociabilis 7	0.333	*	*	*	*
B) Population bottleneck tests for *C. haigi*					
Sociabilis 1	1.000	0.713	0.634	0.599	0.583
Sociabilis 4	1.000	-	-	-	-
Sociabilis 5	0.538	*	*	*	*
Sociabilis 6	0.727	-	-	-	-
Sociabilis 7	0.750	-	-	-	-

Modeling of demographic parameters.—Serial Bayesian coalescent modeling based on demographic data from *C. sociabilis* revealed that observed patterns of pre- and post-eruption microsatellite variation differed between our empirical data and expected outcomes based on our demographic models ($P < 0.05$). This finding suggests that the observed post-eruption increase in microsatellite diversity in *C. sociabilis* was contrary to predictions based on the demography of this species.

Application of an ABC modeling framework to our simulated microsatellite distributions revealed that the MLEs of N_e for the focal population of *C. sociabilis* ranged from 244 to 254 (Fig. 4A); these values are 4 to 5 times greater than empirical estimates of N_e for this population (E. A. Lacey, pers. obs.), suggesting that the increase in N_e required to generate the observed post-eruption increase in microsatellite diversity is biologically unlikely. The MLEs for microsatellite mutation rate ranged from 0.0153 to 0.0165 (Fig. 4B); again, these rates fall beyond the range of mutation rates considered biologically likely for microsatellites (10^{-3} to 10^{-4}—Mapelli et al. 2012), suggesting that mutation cannot account for the post-eruption increase in diversity observed in *C. sociabilis*. When data from the pooled ancillary populations were included in these simulations, posterior distributions revealed a better fit (sharp peaks in posterior distributions, lower delta scores) when migration from the focal population to other populations was allowed (for clarity, all migration rates are presented as going forward in time, although simulations were run backward in time). The fit of posterior distributions increased as the rate of migration from the focal population to other populations was increased or N_e for the pooled additional populations was increased. Indeed, even a modest migration rate of 0.01 (1% probability per generation for each individual migrating from the focal to the pooled ancillary population), along with a small effective size ($N_e = 50$) for the pooled ancillary population produced a peak indicating a MLE of 0.075 for migration into the focal population. Overall, MLEs for migration rate into the focal population ranged from 0.0176 to 0.075 (Fig. 5), which represents a maximum migration of 4.5 individuals per generation, a number that is biologically plausible for this species (Lacey and Wieczorek 2004).

Discussion

Our analyses indicate that the 2011 eruption of the Puyehue-Cordón Caulle volcanic complex in southern Chile impacted genetic variation in *C. sociabilis* and that the consequences of this event differed between the group-living *C. sociabilis* and the parapatric, solitary *C. haigi*. Long-term behavioral and demographic studies of a population of each species located within the area of ash fall revealed significant reductions in population density in both taxa during the 1st summer breeding season following the eruption (E. A. Lacey, pers. obs.). Such demographic bottlenecks are typically expected to result in a loss of genetic variation (England et al. 2003).

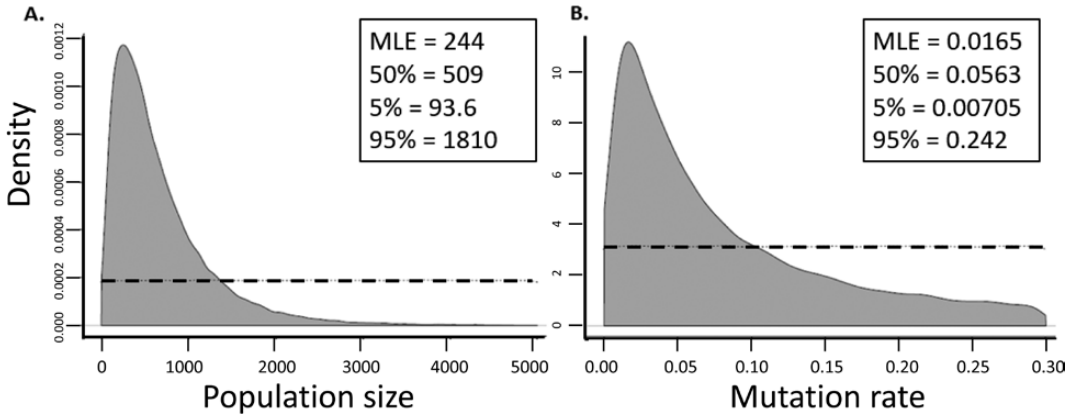

Fig. 4.—Posterior distributions (in gray) for A) current, post-eruption effective population size and B) mutation rate. Both distributions were generated using an approximate Bayesian computation framework from 1,000,000 simulations run by Bayesian serial coalescent modeling. In each panel, the dashed line indicates the uniform distribution used as a prior distribution. Four mean summary statistics from the empirical data were used: observed heterozygosity before and after the 2011 eruption and allelic variance before and after the 2011 eruption. Posterior distributions for both N_e and mutation rate display sharp peaks for most likely estimate (MLE) values, indicating high confidence in these values.

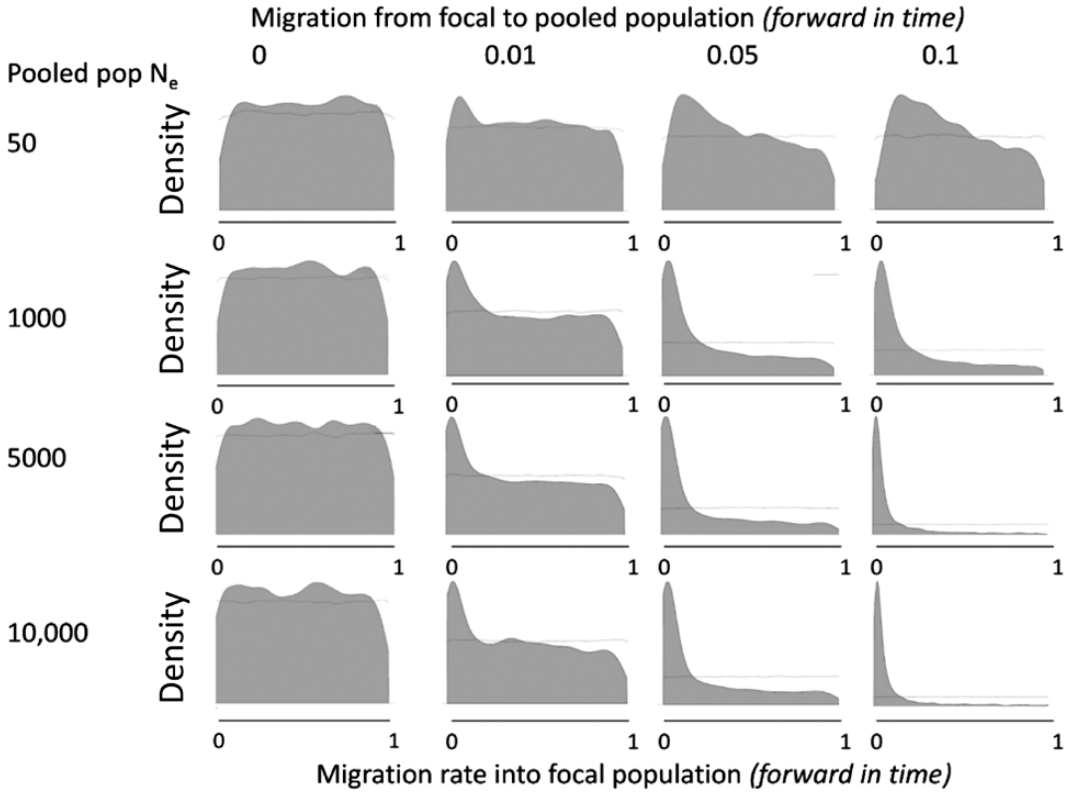

Fig. 5.—Posterior distributions for migration from the collective, pooled ancillary populations of *Ctenomys sociabilis* populations into the focal population of this species, as represented forward in time (all simulations were run backward in time but are presented here as forward in time for clarity). The prior for this migration was set as a uniform distribution from 0 to 1 in all simulations. Migration rate is represented on the x-axis, with the scale from 0 to 1 in each graph (see line on bottom left presenting a representative x-axis). Density is depicted on the y-axis (scale varies) and reflect relative probability. Sharper peaks indicate better fit for each model.

However, contrary to this expectation, we found no evidence of a post-eruption decrease in variation at the mitochondrial cytochrome *b* locus or multiple microsatellite loci in either *C. sociabilis* or *C. haigi*. Instead, our analyses revealed that observed heterozygosity at multiple microsatellite loci was greater in *C. sociabilis*, but not in *C. haigi*, after the 2011 eruption. This apparent post-eruption increase in genetic variation in *C. sociabilis* is intriguing, particularly given the overall low levels of genetic diversity in mitochondrial genes reported for both modern pre-eruption populations of this species and historical populations dating back to 3,000–5,000 years before present (Lacey 2001; Hadly et al. 2003; Chan et al. 2005). Collectively, these analyses concur in suggesting that *C. sociabilis* appears to have experienced repeated demographic bottlenecks during

its history. The 2011 eruption of the Puyehue-Cordón Caulle complex, however, did not result in an immediate loss of microsatellite genetic diversity but instead led to an unexpected increase in local genetic diversity.

Power of analyses to detect genetic differentiation.—Our analyses were based on data from the mitochondrial cytochrome *b* locus and multiple microsatellite loci. While we expected the 2011 eruption to have caused decreases in genetic variation, the failure to detect post-eruption changes in cytochrome *b* in *C. sociabilis* is unsurprising given that only 1 cytochrome *b* haplotype was present in the focal population of this species prior to the eruption and that variation at this locus appears to have been limited to this single haplotype for at least the past 1,000 years, meaning that there could be no further reduction in genetic variation at this locus (Hadly et al. 2003). Similarly, we find no evidence of a post-eruption decrease in genetic variation in the focal population of *C. haigi*, although such a decrease was possible due to the multiple cytochrome *b* haplotypes present before the eruption. The ability to infer demographic events from changes in variation at a single locus may be limited, however, as not all portions of the genome are equally capable of capturing the effects of recent demographic events (Matocq and Villablanca 2001; Kilian et al. 2007). The limitations of examining a single mitochondrial gene, combined with a smaller number of individuals sampled in *C. haigi* ($n = 17$), may explain the lack of a signal in cytochrome *b* for a post-eruption population decline in this species.

In addition, although our microsatellite analyses are based on a relatively limited number of loci, the results of our POWSIM analyses indicated that these data should have provided sufficient statistical power to detect pre- and post-eruption differences in genetic diversity as well as differences between the focal and ancillary populations of the same species. An equivalent number of loci have been used to document population differentiation in other taxa (Hale et al. 2001; Laikre et al. 2005; Ryman and Palm 2006). Similarly, the number of individuals per population sampled should have been sufficient to provide reasonable estimates of genetic variation, given that a threshold of 25–30 individuals (and 15–20 individuals for populations with high polymorphism) has been suggested to be adequate for quantifying genetic diversity using microsatellites (Hale et al. 2012). These lines of evidence, combined with our findings that multiple loci were concordant in suggesting an increase in post-eruption diversity in *C. sociabilis*, lead us to conclude that this outcome is robust and that our results reflect overall trends in genetic variation in our study species.

Evidence of bottlenecks and past demographic change.—Our analyses of microsatellite data revealed interspecific differences in the signals for past bottlenecks. Both analyses of heterozygosity excess and *M*-ratio values consistently indicated a past bottleneck in the focal population of *C. sociabilis*. In contrast, no such evidence of past reductions in population size was obtained for the focal population of *C. haigi*. Although this outcome may at first seem incompatible with the documented decrease in population density in both species and the post-eruption increase in microsatellite variation detected for *C. sociabilis*, these tests are best able to detect bottlenecks occurring between 10 and as far as 50 generations ago (Peery et al. 2012). As such, genetic signals of reductions in population size may not become apparent immediately following such an event (Peery et al. 2012; Hoban et al. 2013), suggesting that our evidence for bottlenecks in *C. sociabilis* may reflect demographic changes occurring prior to this study. Indeed, such bottleneck tests have been demonstrated to be most likely to detect ancient bottlenecks resulting in moderate to severe declines in population size (Girod et al. 2011). Consistent with this, *M*-ratio tests of microsatellite data from the same focal population during the pre-eruption period have shown signals of such a bottleneck (Lacey 2001), and paleogenetic data along with Bayesian modeling have provided evidence for a severe bottleneck within the past 3,000 years (Hadly et al. 2003; Chan et al. 2006). Thus, it seems likely that the evidence of reductions in population size in *C. sociabilis* reported here reflect older demographic events and not the impacts of the 2011 volcanic eruption.

Interspecific differences in genetic response.—Several factors may have contributed to the apparent interspecific differences in genetic response to the 2011 eruption reported here. Possibilities include a difference in the deposition of ash between the focal populations of the study species. Although these populations are located immediately across the Limay River from each other, ash depth was greater at the *C. sociabilis* study site (E. A. Lacey, pers. obs.). As a result, the consequences of the eruption may have been more severe for *C. sociabilis*. At the same time, the 2 species differ markedly with respect to behavior and demography (Lacey et al. 1997, 1998; Lacey and Wieczorek 2004) and these differences may have contributed to the differential genetic responses reported here. In particular, *C. sociabilis* is group living, with multiple closely related adult females sharing the same burrow system and rearing their young communally (Lacey et al. 1997; Izquierdo and Lacey 2008). Groups form due to natal philopatry by females and although all males disperse from their natal burrows, movement of these animals is often within the same local population (Lacey and Wieczorek 2004). In contrast, *C. haigi* is solitary, with individuals of both sexes dispersing from their natal burrow (Lacey et al. 1998). These differences in social behavior and associated dispersal patterns suggest that migration among populations is typically more common in *C. haigi*, which likely contributed to the substantially greater pre-eruption levels of microsatellite diversity in the focal population of this species (Lacey 2001). Together, this background of greater pre-eruption genetic diversity and the presumably higher rates of migration and gene flow among local populations may have served to minimize the impacts of the 2011 eruption on microsatellite diversity in *C. haigi* as compared to *C. sociabilis*.

Demography and increased post-eruption genetic variation.—The most striking result revealed by our analyses—the apparently greater post-eruption microsatellite variation in *C. sociabilis*—may reflect changes in multiple demographic processes, including drift, mutation, and selection. Each of these processes could influence genetic diversity following a population decline.

Our analyses, however, indicate that these factors are unlikely to explain the observed post-eruption change in genetic diversity in *C. sociabilis*. First, our Bayesian modeling demonstrates that our microsatellite results do not fit the expected window of change given random genetic drift (and absent selection, mutation, and migration) after such a demographic bottleneck. In addition, such modeling suggests that a much larger population size than is observed empirically is required to maintain the level of genetic variation observed. Second, these analyses indicate that the mutation rates required to produce the observed change in variation exceed empirical limits for microsatellite loci (Mapelli et al. 2012). Although increased mutation rates have been reported following some catastrophic environmental events, these reports appear to be limited to environmental changes involving known mutagens (e.g., radiation from the Chernobyl nuclear disaster—Dubrova et al. 1996; Ellegren et al. 1997). Third, microsatellites are considered putatively neutral (Li et al. 2002), and given the timescales and putatively random mortality caused by the bottleneck it is unlikely that balancing selection plays a major role following the 2011 eruption. Thus, we suggest that genetic drift, mutation, and selection in the microsatellite loci cannot individually account for the post-eruption changes in genetic diversity in *C. sociabilis*.

Instead, the increase in microsatellite variation reported here for *C. sociabilis* is most consistent with a scenario of enhanced post-eruption migration and gene flow. Nearby populations of this species may possess different genetic variants, and migration (and thus gene flow) from such populations could have contributed to the observed greater post-eruption genetic diversity in the focal study population. This hypothesis is supported by our demographic modeling, which indicates that the observed increase in variation was unlikely in the absence of migration. Increasing simulated migration rates among nearby populations produced a predicted increase in variation similar to that observed in our empirical data set. Although we do not have the power to ascertain the precise rate of migration that occurred after the 2011 eruption given that effective population sizes for the neighboring populations are unknown, our modeling demonstrates that even small amounts of migration from nearby populations could lead to the levels of increased genetic diversity in the focal population. As such, our results suggest an increase in gene flow from other *C. sociabilis* populations following the 2011 eruption. The ancillary locations sampled (Fig. 1) are all located in close proximity (< 1 km) to the focal *C. sociabilis* population, with no apparent geographic barriers between populations. Our estimates for the range of migration rates needed to generate the observed post-eruption change in genetic variation are biologically plausible for *C. sociabilis* (Lacey and Wieczorek 2004), and dispersal events occurring over 1–2 km have been detected for this species (E. A. Lacey, pers. obs.). Such movements are also consistent with patterns of dispersal, migration, and gene flow found in other ctenomyids (Fernández-Stolz et al. 2007; Lopes and De Freitas 2012; Roratto et al. 2015). Additionally, this hypothesis is also consistent with the increased percentage of unmarked (potentially immigrant) females captured in the focal study population of *C. sociabilis* during the breeding season following the eruption (E. A. Lacey, pers. obs.). Thus, based on demographic models and empirical data, post-eruption migration and gene flow among local populations appear to provide the most logical explanation for the observed increase in microsatellite genetic diversity in *C. sociabilis*.

Implications for studies of environmental catastrophes.—Our findings suggest that short-term migration among local populations can play an important role in determining levels of genetic diversity immediately following catastrophic environmental events. In particular, such migration may serve to mitigate expected declines in genetic diversity associated with reductions in effective population size. Increases in local genetic diversity after reductions in population size have been documented for other species, including montane voles (*Microtus montanus*—Hadly et al. 2004) and artesian spring snails (*Fonscochlea accepta*—Wilmer et al. 2011); enhanced migration and gene flow have been suggested as the most likely explanation for these findings. Thus, while catastrophic environmental events are typically expected to result in population bottlenecks and reductions in genetic diversity, actual responses to such changes may be more complex and result in different genetic outcomes. Determining how a given species will respond to such events is challenging and requires detailed information regarding both the nature and magnitude of the environmental change as well detailed information regarding the demography of the organisms in question. As documented here, the 2011 eruption of the Puyehue-Cordón Caulle complex produced different genetic responses in *C. sociabilis* and *C. haigi*, with post-eruption microsatellite heterozygosity increasing in the former species but not the latter. Over the past few thousand years, however, *C. sociabilis* has experienced a decline in genetic variation that is not evident in *C. haigi* (Chan et al. 2005; Chan and Hadly 2011), thereby underscoring the variable nature of responses to environmental conditions. These differences in response—both between species and time periods—raise intriguing questions regarding how interactions among environmental changes, demography, and existing levels of genetic diversity interact to shape responses to a given catastrophic event. We expect migration and gene flow to be an important part of this equation and thus opportunities to combine detailed demographic information with genetic data should prove important in understanding and predicting response to environmental change.

Acknowledgments

We thank K. Solari, S. Redondo, J. Flanders, A. Mychajliw, E. López, and other members of the Hadly lab for helpful comments. H. Fraser, S. Palumbi, U. Ramakrishnan, and N. Rosenberg also provided invaluable feedback. We also thank the Delegacion Tecnica Regional Patagonica de Parques Nacionales Argentinas and Provincia Rio Negro, Argentina, for assistance in obtaining permits. This work is funded by NSF RAPID grant DEB-1201541 (EAH, EAL) and a Stanford Center for Computational, Evolutionary, and Human Genomics

trainee grant (JLH). JLH is supported by NSF Graduate Research Fellowship and Stanford Graduate Fellowship, MNT was supported by a CONICET Predoctoral Fellowship, and SK received support from the Stanford Vice Provost for Undergraduate Education.

Supplementary Data

Supplementary data are available at *Journal of Mammalogy* online.

Supplementary data SD1.—Haplotypic networks throughout the past 12,000 years for A) 398 base pairs of cytochrome *b* in *C. sociabilis* and B) 388 base pairs of cytochrome *b* in *C. haigi*. These network maps represent haplotypic change temporally, with the bottom layers reflecting haplotype networks in the past (from ancient DNA) and the top layers reflecting modern diversity.

Literature Cited

Akey, J. M., et al. 2004. Population history and natural selection shape patterns of genetic variation in 132 genes. PLoS Biology 2:e286.

Anderson, C. N., U. Ramakrishnan, Y. L. Chan, and E. A. Hadly. 2005. Serial simcoal: a population genetics model for data from multiple populations and points in time. Bioinformatics 21:1733–1734.

Beheregaray, L. B., C. Ciofi, D. Geist, J. P. Gibbs, A. Caccone, and J. R. Powell. 2003. Genes record a prehistoric volcano eruption in the galápagos. Science 302:75.

Boretto, J., F. Cabezas-Cartes, and E. Kubisch. 2014. Changes in female reproduction and body condition in an endemic lizard, *Phymaturus spectabilis*, following the Puyehue volcanic ashfall event. Herpetological Conservation and Biology 9:181–191.

Chan, Y. L., C. N. K. Anderson, and E. A. Hadly. 2006. Bayesian estimation of the timing and severity of a population bottleneck from ancient DNA. PLoS Genetics 2:451–460.

Chan, Y. L., and E. A. Hadly. 2011. Genetic variation over 10,000 years in *Ctenomys*: comparative phylochronology provides a temporal perspective on rarity, environmental change and demography. Molecular Ecology 20:4592–4605.

Chan, Y. L., E. A. Lacey, O. P. Pearson, and E. A. Hadly. 2005. Ancient DNA reveals Holocene loss of genetic diversity in a South American rodent. Biology Letters 1:423–426.

Cohen, J. 1988. Statistical power analysis for the behavioral sciences. 2nd ed. Laurence Erlbaum Associates, Hillsdale, New Jersey.

Collini, E., M. S. Osores, A. Folch, J. G. Viramonte, G. Villarosa, and G. Salmuni. 2012. Volcanic ash forecast during the June 2011 Cordón Caulle eruption. Natural Hazards 66:389–412.

Cornuet, J. M., and G. Luikart. 1996. Description and power analysis of two tests for detecting recent population bottlenecks from allele frequency data. Genetics 144:2001–2014.

Dubrova, Y. E., et al. 1996. Human minisatellite mutation rate after the Chernobyl accident. Nature 380:683–686.

Ellegren, H., G. Lindgren, C. R. Primmer, and A. P. Møller. 1997. Fitness loss and germline mutations in barn swallows breeding in Chernobyl. Nature 389:593–596.

England, P., G. Osler, M. Woodworth, M. Mongomery, D. Briscoe, and R. Frankham. 2003. Effects of intense versus diffuse population bottlenecks on microsatellite genetic diversity and evolutionary potential. Conservation Genetics 4:595–604.

Excoffier, L., and G. Laval. 2005. Arlequin (version 3.0): an integrated software package for population genetics data analysis. Evolutionary Bioinformatics 1:47–50.

Fernández-Stolz, G. P., J. F. B. Stolz, and T. R. O. De Freitas. 2007. Bottlenecks and dispersal in the Tuco-Tuco Das Dunas, *Ctenomys flamarioni* (Rodentia: Ctenomyidae), in Southern Brazil. Journal of Mammalogy 88:935–945.

Flueck, W. T., and J. A. Smith-Flueck. 2013. Severe dental fluorosis in juvenile deer linked to a recent volcanic eruption in Patagonia. Journal of Wildlife Diseases 49:355–366.

Flueck, W., J. Smith-Flueck, B. Mincher, and L. Winkel. 2014. An alternative interpretation of plasma selenium data from endangered Patagonian huemul deer (*Hippocamelus bisulcus*). Journal of Wildlife Diseases 50:1003–1004.

Funk, W., E. Forsman, M. Johnson, T. Mullins, and S. Haig. 2010. Evidence for recent population bottlenecks in northern spotted owls (*Strix occidentalis caurina*). Conservation Genetics 11:1013–1021.

Gaitán, J. J., J. A. Ayesa, F. Raffo, F. Umaña, D. B. Bran, and H. Moraga. 2011. Monitoreo de la distribución de cenizas volcánicas en Río Negro y Neuquén: Situación a los 6 meses de la erupción, Rep., 12 pp., Instituto Nacional de Tecnología Agropecuaria (INTA), San Carlos de Bariloche, Argentina.

Garza, J. C., and E. G. Williamson. 2001. Detection of reduction in population size using data from microsatellite loci. Molecular Ecology 10:305–318.

Girod, C., R. Vitalis, R. Leblois, and H. Fréville. 2011. Inferring population decline and expansion from microsatellite data: a simulation-based evaluation of the msvar method. Genetics 188:165–179.

Goudet, J. 1995. FSTAT (version 1.2): a computer program to calculate F-statistics. Journal of Heredity 86:485–486.

Hadly, E. A., et al. 2004. Genetic response to climatic change: insights from ancient DNA and phylochronology. PLoS Biology 2:e290.

Hadly, E. A., M. Van Tuinen, Y. Chan, and K. Heiman. 2003. Ancient DNA evidence of prolonged population persistence with negligible genetic diversity in an endemic tuco-tuco (*Ctenomys sociabilis*). Journal of Mammalogy 84:403–417.

Hale, M., R. Bevan, and K. Wolff. 2001. New polymorphic microsatellite markers for the red squirrel (*Sciurus vulgaris*) and their applicability to the grey squirrel (*S. carolinensis*). Molecular Ecology Notes 1:47–49.

Hale, M., T. Burg, and T. Steeves. 2012. Sampling for microsatellite-based population genetic studies: 25 to 30 individuals per population is enough to accurately estimate allele frequencies. PLoS One 7:e45170.

Hoban, S., O. Gaggiotti, and G. Bertorelle. 2013. The number of markers and samples needed for detecting bottlenecks under realistic scenarios, with and without recovery: a simulation-based study. Molecular Ecology 22:3444–3450.

Izquierdo, G., and E. Lacey. 2008. Effects of group size on nest attendance in the communally breeding colonial tuco-tuco. Mammalian Biology 73:438–443.

Kilian, B., et al. 2007. Molecular diversity at 18 loci in 321 wild and 92 domesticate lines reveal no reduction of nucleotide diversity during *Triticum monococcum* (einkorn) domestication: implications for the origin of agriculture. Molecular Biology and Evolution 24:2657–2668.

Lacey, E. A. 2001. Microsatellite variation in solitary and social tuco-tucos: molecular properties and population dynamics. Heredity 86:628–637.

Lacey, E., S. Braude, and J. Wieczorek. 1997. Burrow sharing by colonial tuco-tucos (*Ctenomys sociabilis*). Journal of Mammalogy 78:556–562.

Lacey, E. A., S. H. Braude, and J. R. Wieczorek. 1998. Solitary burrow use by adult Patagonian tuco-tucos (*Ctenomys haigi*). Journal of Mammalogy 79:986–991.

Lacey, E. A., and L. A. Ebensperger. 2007. Social structure in Octodontid and Ctenomyid rodents. Pp. 403–415 in Rodent societies: an ecological and evolutionary perspective (J. O. Wolff and P. W. Sherman, eds.). University of Chicago Press, Chicago, Illinois.

Lacey, E. A., J. E. Maldonado, J. P. Clabaugh, and M. D. Matocq. 1999. Interspecific variation in microsatellites isolated from tuco-tucos (Rodentia: Ctenomyidae). Molecular Ecology 8:1754–1756.

Lacey, E. A., and J. R. Wieczorek. 2004. Kinship in colonial tuco-tucos: evidence from group composition and population structure. Behavioral Ecology 15:988–996.

Laikre, L., et al. 2005. Spatial genetic structure of northern pike (*Esox lucius*) in the Baltic Sea. Molecular Ecology 14:1955–1964.

Lallement, M., S. Juárez, P. Macchi, and P. Vigliano. 2014. Puyehue Cordón-Caulle: post-eruption analysis of changes in stream benthic fauna of Patagonia. Ecología Austral 24:64–74.

Li, Y. C., A. B. Korol, T. Fahima, A. Beiles, and E. Nevo. 2002. Microsatellites: genomic distribution, putative functions and mutational mechanisms: a review. Molecular Ecology 11:2453–2465.

Lopes, C. M., and T. R. De Freitas. 2012. Human impact in naturally patched small populations: genetic structure and conservation of the burrowing rodent, tuco-tuco (*Ctenomys lami*). The Journal of Heredity 103:672–681.

Mapelli, F., M. Mora, P. Mirol, and M. Kittlein. 2012. Population structure and landscape genetics in the endangered subterranean rodent *Ctenomys porteousi*. Conservation Genetics 13:165–181.

Masciocchi, M., A. J. Pereira, M. V. Lantschner, and J. C. Corley. 2012. Of volcanoes and insects: the impact of the Puyehue–Cordon Caulle ash fall on populations of invasive social wasps, *Vespula* spp. Ecological Research 28:199–205.

Matocq, M. D., and F. X. Villablanca. 2001. Low genetic diversity in an endangered species: recent or historic pattern? Biological Conservation 98:61–68.

Morales, C., A. Saez, M. Arbetman, L. Cavallero, and M. Aizen. 2014. Detrimental effects of volcanic ash deposition on bee fauna and plant-pollinator interactions. Ecología Austral 24:42–50.

Peery, M. Z., et al. 2012. Reliability of genetic bottleneck tests for detecting recent population declines. Molecular Ecology 21:3403–3418.

Piry, S. 1999. Computer note. BOTTLENECK: a computer program for detecting recent reductions in the effective size using allele frequency data. Journal of Heredity 90:502–503.

Prost, S., and C. Anderson. 2011. TempNet: a method to display statistical parsimony networks for heterochronous DNA sequence data. Methods in Ecology and Evolution 2:663–667.

Pujolar, J. M., S. Vincenzi, L. Zane, D. Jesensek, G. A. De Leo, and A. J. Crivelli. 2011. The effect of recurrent floods on genetic composition of marble trout populations. PLoS One 6:e23822.

Raymond, M., and F. Rousset. 1995. GENEPOP (version 1.2): population genetics software for exact tests and ecumenicism. Journal of Heredity 86:248–249.

Roratto, P. A., F. A. Fernandes, and T. R. O. De Freitas. 2015. Phylogeography of the subterranean rodent *Ctenomys torquatus*: an evaluation of the riverine barrier hypothesis. Journal of Biogeography 42:694–705.

Ryman, N., and S. Palm. 2006. POWSIM: a computer program for assessing statistical power when testing for genetic differentiation. Molecular Ecology Notes 6:600–602.

Sikes, R. S., and The Animal Care and Use Committee of the American Society of Mammalogists. 2016. 2016 Guidelines of the American Society of Mammalogists for the use of wild mammals in research and education. Journal of Mammalogy 97:663–688.

Smith, M. F. 1998. Phylogenetic relationships and geographic structure in pocket gophers in the genus *Thomomys*. Molecular Phylogenetics and Evolution 9:1–14.

Tajima, F. 1983. Evolutionary relationship of DNA sequences in finite populations. Genetics 105:437–460.

Van Oosterhout, C., W. Hutchinson, D. Wills, and P. Shipley. 2004. MICRO-CHECKER: software for identifying and correcting genotyping errors in microsatellite data. Molecular Ecology Notes 4:535–538.

Watterson, G. A. 1975. On the number of segregating sites in genetical models without recombination. Theoretical Population Biology 7:256–276.

Wilmer, J. W., L. Murray, C. Elkin, C. Wilcox, D. Niejalke, and H. Possingham. 2011. Catastrophic floods may pave the way for increased genetic diversity in endemic artesian spring snail populations. PLoS One 6:e28645.

Wilson, T., et al. 2012. Impactos en la salud y el medioambiente producidos por la erupción del Complejo Volcánico Puyehue-Cordón Caulle del 4 de Junio de 2011: Informe de un equipo de investigación multidisciplinario. 25 pp.

Wilson, T., et al. 2013. Impacts of the June 2011 Puyehue-Cordón Caulle volcanic complex eruption on urban infrastructure, agriculture and public health, 22 pp., GNS Science Report 2012/20.

Yue, G., P. Beeckmann, and H. Geldermann. 2002. Mutation rate at swine microsatellite loci. Genetica 114:113–119.

Submitted 16 August 2016. Accepted 25 January 2017.

Associate Editor was Jessica Light.